Emergent fault friction in a continuum model of rupture

Abhishek Arora* Amit Acharya† Jacobo Bielak‡

Abstract

We model static fault friction − an important physical observation in rupture dynamics, using field dislocation mechanics (FDM). The energy density function in our model encodes accepted, simple physical facts related to rocks and granular materials under compression. We work within a 2-dimensional ansatz of FDM where the rupture front is allowed to move only in a horizontal fault layer sandwiched between elastic blocks. Elastic damage is allowed to occur only in the fault layer, characterised by the amount of plastic slip. The theory dictates the evolution equation of the plastic shear strain to be a Hamilton-Jacobi (H-J) equation, resulting in the representation of a propagating rupture front. A Central-Upwind scheme is used to solve the H-J equation. The rupture propagation is fully coupled to elastodynamics in the whole domain, and our simulations recover static friction laws as emergent features of our continuum model, without putting in by hand any discontinuous, "off-on" switching criterion. We fit a linear curve (which resembles the Mohr–Coulomb failure curve) to our simulation data, and make a quantitative prediction of material constants for rocks like cohesion and friction angle.

1 Introduction

We model the important physical observation of static fault friction in dynamic rupture. A rupture may be considered as the study of two large blocks of material slipping with respect to each other over a thin region, which is very small as compared to the size of blocks. Conventionally, rupture dynamics has been studied as a problem of friction between two bodies. A crack is assumed to exist behind the rupture front, and the crack faces transmit shear and normal stresses, where the amount of shear stress transmitted is governed by an *assumed* friction law and is assumed to be continuous across the crack surface. It has been historically suggested that dynamic rupture may be studied using the framework of a dislocation propagating in a slip plane [Bru70, Nab87]. However, it is important to note some key differences between a classical dislocation and a crack-like model for rupture. For a dislocation in an elastic medium, there is a displacement discontinuity of fixed magnitude behind the dislocation line. The stresses transmitted across the slipped region are not limited in principle, but have to be continuous, except at the core singularity. Moreover, the classical theory of dislocations and its solution techniques do not allow for incorporating damage in the wake of the dislocation line, which is essential for modeling a rupture using dislocation theory. Recently, Zhang et al. [ZAWB15] used a partial differential equation (pde) based framework called field dislocation mechanics (FDM) to study dynamic rupture. They were able to predict short-slip duration from their simulations by allowing for appropriate amount of elastic damage, i.e. degradation in elastic modulus, behind the front. Conventionally, short-slip duration is predicted

*Department of Civil & Environmental Engineering, Carnegie Mellon University, Pittsburgh, PA 15213.

†Department of Civil & Environmental Engineering, and Center for Nonlinear Analysis, Carnegie Mellon University, Pittsburgh, PA 15213, email: acharyaamit@cmu.edu.

‡Department of Civil & Environmental Engineering, Carnegie Mellon University, Pittsburgh, PA 15213.

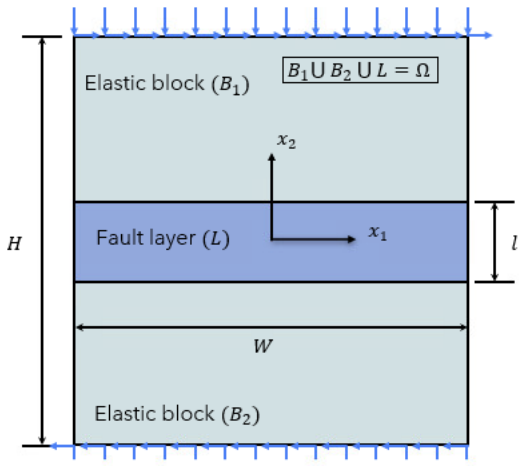

Figure 1: A schematic of a fault layer surrounded by elastic blocks and under transverse plus compressive loading.

using assumed slip velocity-weakening friction laws based on the physical phenomenon of self-healing, as suggested by [Hea90], and later explored in [Ric01].

In their work, Zhang et al. [ZAWB15] utilised an ansatz to produce an exact, reduced and planar model of FDM, where the dislocations/rupture front are allowed to move in a planar fault layer (which is sandwiched between elastic blocks), as shown in Fig. 1. The amount of slip during rupture in the model is characterised by the plastic shear strain, and an evolution equation for plastic shear strain can be derived by localising the statement of the conservation of topological charge carried by a defect line, as derived for dislocations [Mur63, Ach11], or for a crack-tip [Ach18]. Finally, the evolution equation obtained for the plastic shear strain is an Hamilton-Jacobi (H-J) equation and it enables the representation of a propagating rupture front. The plastic shear strain in the fault layer is assumed to induce elastic damage behind the rupture front, and with elastic blocks remaining undamaged. This leads to an energetic driving force contribution for the evolution of plastic strain, that was noted, but not accounted for, in the rupture-related simulations in [ZAWB15].

Friction is the physical phenomenon where the slipping between two blocks is restricted up to some applied transverse force, with pressure being imposed upon the blocks. In context of geo-materials, frictional behavior is interpreted in terms of stresses and not in terms of forces, as in conventional observations of friction.

In the context of a fault layer sandwiched between elastic blocks, such thresholds for shear stresses may exist, as one may expect motion of the front only after sufficient energy has been provided to induce damage in the undamaged region ahead of the damage/rupture front.

We extend here the formulation of FDM [ZAWB15] to model a propagating rupture front in the fault layer. We study fault friction and show that it emerges as a feature of our continuum model, although, there are no *discontinuous* "on-off" criteria put in by hand in our model.

The main physical assumptions built into our model are as follows:

- It is assumed that fault layer responds to compressive elastic strain with intact compressive elastic stiffness, a characteristic of geomaterials.

- There is an energetic cost required to induce elastic damage in the rupture front, which is modeled by a *damage* energy density function (η), shown in Fig. 2. It is composed of two parts

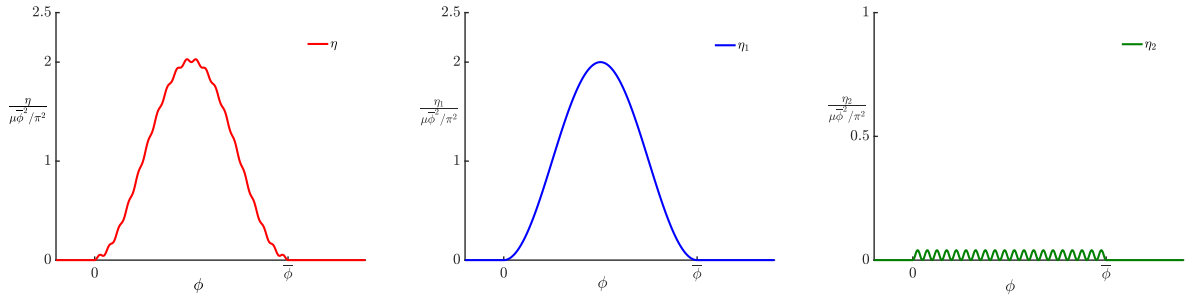

(a) $\eta = \eta_1 + \eta_2$ (b) η_1 (c) η_2

Figure 2: A typical damage energy function in our model.

(η_1 and η_2), and η_1 models the fact that the damage energy required to cause motion increases only up to some value of slip/plastic strain. Hence, it monotonically increases, and then decreases, and eventually becomes zero after a certain level of plastic strain is achieved. The η_2 function has small perturbations, with amplitude proportional to compressive elastic strain, the latter reflecting the fact that geomaterials have higher strength in compression. It also vanishes after the previously mentioned plastic strain/damage threshold (refer to Fig. 2(c)). This models the cyclic gain/loss in the strength of geomaterials due to rearrangement of their 'fabric' [CS79, Beh15]. We show later in our results that such small, high frequency perturbations have a significant impact on the fault dynamics and the prediction of pressure dependence of the strength against rupture of the fault.

- The rupture front velocity is assumed to be proportional to its theoretically derived driving force as shown Sec. 2, a suffcient condition for the model to be in accord with the second law of thermodynamics. For a self-consistent evolution of a propagating rupture front, we account for the additional energetic driving force, mentioned earlier.

In order to numerically solve the H-J equation, we utilise an implementation of a semi-discrete version of the Central-Upwind scheme developed by [KNP01].

In related work, a field crack mechanics model [MA21] was developed recently to model brittle crack propagation in elastic bodies. A key difference of that work from ours is that there is no internal stress due to a dislocation defect. However, the compressive elastic stiffness in the fault layer remains intact under compressive strain, as assumed here.

With regard to relevant work for friction, Ruina [Rui83] studied slip instability for friction laws dependent upon state variables like slip rate, slip distance and time-dependent static friction. Ruina et al. [RKCH86] did theoretical and experimental work related to frictional behavior of rocks at low normal stress. These aspects of material response are important in understanding the size, nature and even existence of earthquakes, if modeled using slip instabilities. Recently, Hulikal et al. [HLB18] studied static and sliding contact between rough surfaces. They model the contact between two surfaces using discrete deformable elements attached to elastic blocks and these elements are elasto/viscoplastic springs.

The outline of this paper is as follows: the following paragraph contains some notational details. Section 2 discusses the details of our mathematical model for a rupture front in the fault layer, while Section 3 outlines the numerical schemes used for solving the governing equations in our model. In Section 4, we show that our simulations recover static friction laws as emergent features of our

continuum model, also resembling the Mohr–Coulomb failure criterion for geomaterials, including well-defined features of cohesion and friction angle. Section 5 presents some concluding remarks along with future directions for research.

Vectors and tensors are represented by bold face lower and upper-case letters. The action of a second order tensor $\boldsymbol{A}$ on a vector $\boldsymbol{b}$ is denoted by $\boldsymbol{Ab}$. The inner product of two vectors is denoted by $\boldsymbol{a}\cdot\boldsymbol{b}$, while the inner product of two second order tensors is denoted by $\boldsymbol{A}:\boldsymbol{B}$. A rectangular Cartesian coordinate system is invoked for ambient space and all (vector) tensor components are expressed with respect to the basis of this coordinate system. $(\cdot)_{,i}$ denotes the partial derivative of the quantity $(\cdot)$ w.r.t. the x_i coordinate of this coordinate system. $\boldsymbol{e}_i$ denotes the unit vector in the x_i direction. The time derivative of a quantity is denoted by $\dot{(\cdot)}$. Einstein's summation convection is always implied, unless mentioned otherwise. The symbols grad, div, and curl denote the gradient, divergence, and curl on the current configuration. For a second order tensor $\boldsymbol{A}$, vectors $\boldsymbol{v}$, $\boldsymbol{a}$, and $\boldsymbol{c}$, a spatially constant vector field $\boldsymbol{b}$, the operations of div, curl, and cross-product of a tensor $(\times)$ with a vector are defined as follows:

$$\begin{aligned}(\operatorname{div}\boldsymbol{A})\cdot\boldsymbol{b} &= \operatorname{div}\left(\boldsymbol{A}^T\boldsymbol{b}\right), &&\forall\ \boldsymbol{b}\\ \boldsymbol{b}\cdot(\operatorname{curl}\boldsymbol{A})\,\boldsymbol{c} &= \left[\operatorname{curl}\left(\boldsymbol{A}^T\boldsymbol{b}\right)\right]\cdot\boldsymbol{c}, &&\forall\ \boldsymbol{b},\boldsymbol{c}\\ \boldsymbol{c}\cdot(\boldsymbol{A}\times\boldsymbol{v})\,\boldsymbol{a} &= \left[\left(\boldsymbol{A}^T\boldsymbol{c}\right)\times\boldsymbol{v}\right]\cdot\boldsymbol{a}. &&\forall\ \boldsymbol{a},\boldsymbol{c}\end{aligned}$$

In rectangular Cartesian coordinates, these are denoted by

$$(\operatorname{div}\boldsymbol{A})_i = A_{ij,j},\quad (\operatorname{curl}\boldsymbol{A})_{ri} = \varepsilon_{ijk}A_{rk,j},\quad (\boldsymbol{A}\times\boldsymbol{v})_{ri} = \varepsilon_{ijk}A_{rj}v_k,$$

where ε_{ijk} are the components of the third order alternating tensor $\boldsymbol{X}$.

2 Theory

The energy density function in our model has three ingredients i.e. *elastic*, *core* and *damage* energies, and is given by:

$$\psi(\boldsymbol{\epsilon}^e,\boldsymbol{\alpha},\boldsymbol{U}^p)+\eta(\boldsymbol{U}^p,\epsilon^e_{22}), \tag{3}$$

where ψ represents the summation of elastic and core energies, while η is damage energy, represented by a *non-convex* function. We assume here that the elastic energy depends upon the plastic strain $(\boldsymbol{U}^p)$ as well, in addition to elastic strain $(\boldsymbol{\epsilon}^e)$, as the plastic straining induces damage which degrades the elastic moduli behind the rupture front. The core energy is an energetic penalty penalizing the sharpness of the rupture front, as the completely slipped or un-slipped fault layer is energetically preferred by the damage term. As discussed earlier, the damage energy density function is assumed to depend upon the plastic strain and the elastic compressive strain (ϵ^e_{22}), as the strength of the material changes due to the re-arrangement of fabric, only under compressive strain. In (3), $\boldsymbol{\alpha}$ is the Nye's dislocation density tensor. In the fault layer, we utilize the ansatz from [ZAWB15] and assume that the only non-zero plastic strain is:

$$\boldsymbol{U}^p(x,y,t) = U^p_{12}(x,t)\,\boldsymbol{e}_1\otimes\boldsymbol{e}_2 := \phi(x,t)\,\boldsymbol{e}_1\otimes\boldsymbol{e}_2,$$

and this physically affects the slip in the fault layer. Slip is defined as the difference of the displacement along $\boldsymbol{e}_1$ direction (u_1) between the top and bottom boundary of the fault layer.
Using the incompatibility equation for small deformations, we get,

$$\boldsymbol{\alpha}(x,y,t) = -\operatorname{curl}\boldsymbol{U}^p(x,y,t) = -\phi_x(x,t)\,\boldsymbol{e}_1\otimes\boldsymbol{e}_3,$$

and

$$\operatorname{curl} \boldsymbol{\alpha} = \phi_{xx}(x,t)\, \boldsymbol{e}_1 \otimes \boldsymbol{e}_2.$$

Further we assume that the velocity of rupture front in the fault layer is non-zero only along the $\boldsymbol{e}_1$ direction:

$$\boldsymbol{V}(x,y,t) = V_1(x,y,t)\boldsymbol{e_1} := v(x,t)\boldsymbol{e}_1.$$

With the above ansatz, the conservation law for the topological charge of a dislocation i.e., $\dot{\boldsymbol{\alpha}} = -\operatorname{curl}(\boldsymbol{\alpha} \times \boldsymbol{V})$ is simplified as shown below,

$$\phi_t(x,t) = -\phi_x v(x,t)$$

(up to a gradient).

We assume linear elasticity and a quadratic form for the core energy:

$$\psi(\boldsymbol{\epsilon}^e, \boldsymbol{\alpha}, \boldsymbol{U}^p) = \frac{1}{2}\boldsymbol{\epsilon}^e : \mathbb{C} : \boldsymbol{\epsilon}^e + \frac{1}{2}\epsilon|\boldsymbol{\alpha}|^2,$$

where ϵ is a parameter with physical dimensions of stress $\times$ length^2. The elasticity tensor ($\mathbb{C}$) is assumed to be of the following form:

$$\mathbb{C} := \left\{ \begin{array}{ll} \boldsymbol{C}_L, & (\text{in } L) \\ \boldsymbol{C}. & (\text{in } \Omega \backslash L) \end{array} \right\}$$

where L is the fault layer, while Ω is defined as whole domain, as shown in Fig. 1.
Here, the tensor of elastic moduli ($\boldsymbol{C}$) in the elastic blocks ($\Omega \backslash L$) is assumed to be isotropic and can be written in indicial notation as shown below:

$$C_{ijkl} = \lambda \delta_{ij}\delta_{kl} + \mu(\delta_{ik}\delta_{jl} + \delta_{il}\delta_{jk}),$$

where λ and μ are Lame's constants.
The elasticity tensor ($\boldsymbol{C}_L$) in the fault layer (L) is given as:

$$\boldsymbol{C}_L = \left(\tilde{\lambda} - \frac{|\phi|}{\overline{\phi}}\kappa\right)\boldsymbol{C} + (1 - H(\epsilon^e_{22}))\,\frac{|\phi|}{\overline{\phi}}\,\kappa\, C_{2222}\, \boldsymbol{e}_2 \otimes \boldsymbol{e}_2 \otimes \boldsymbol{e}_2 \otimes \boldsymbol{e}_2, \tag{7}$$

where, $0 < \kappa < \tilde{\lambda} < 1$. Here, $\tilde{\lambda}$ simply allows a difference in the elasticity of the intact fault material from the bulk elastic blocks, while κ is a proportionality constant for damage induced in the ruptured regions of the fault layer due to plastic straining. $H(.)$[1] is the step function, and the the second term in (7) allows the compressive elastic modulus in the fault to be intact under compressive strain.

The dissipation is defined as the difference of power supplied by the external forces and the rate of change of free energy and kinetic energy, as shown below:

$$\mathcal{D} = \int_{\partial\Omega} \boldsymbol{t}\cdot\boldsymbol{v}\, dv + \int_{\Omega} \boldsymbol{b}\cdot\boldsymbol{v}\, dv - \frac{d}{dt}\int_L (\psi(\boldsymbol{\epsilon}^e, \boldsymbol{\alpha}, \boldsymbol{U}^p) + \eta(\boldsymbol{U}^p, \epsilon^e_{22}))\, dv - \frac{d}{dt}\int_{\Omega}\left(\frac{1}{2}\rho|\boldsymbol{v}|^2\right) dv,$$

where $\boldsymbol{t}$ is the applied traction on the boundary of the domain, $\boldsymbol{b}$ is the applied body force in the whole domain, $\boldsymbol{v}$ denotes the material velocity, and ρ denotes the mass density.
In the absence of defects and plastic deformation, we obtain the constitutive relation for Cauchy stress as:

$$\boldsymbol{T} = \frac{\partial\psi}{\partial\boldsymbol{\epsilon}^e} + \frac{\partial\eta}{\partial\epsilon^e_{22}}\boldsymbol{e}_2 \otimes \boldsymbol{e}_2.$$

[1] $H(x)$ is defined as: $H(x) = 1$ if $x > 0$, and $H(x) = 0$ if $x <= 0$.

Using the assumptions of the ansatz, the mechanical dissipation simplifies to:

$$\mathcal{D} = \int_L v(x,t) \left\{ \left[T_{12}(x,y,t) - \frac{\partial \eta}{\partial \phi}(x,y,t) - \frac{\partial \psi}{\partial \phi}(x,y,t) + \epsilon \phi_{xx}(x,t) \right] (-\phi_x(x,t)) \right\} dv,$$

as the boundary terms vanish as shown in [ZAWB15]. There are driving forces due to damage energy, elastic energy and core energy, and some are responsible for causing or preventing the motion of the front, under external loads.
We assume the following expression of fault velocity such that it is proportional to the thermodynamically consistent driving force as shown below:

$$v(x,t) := \frac{-1}{B} \left\{ \left[\tau(x,t) - \tau^b(x,t) - \tau^\psi(x,t) + \epsilon \phi_{xx}(x,t) \right] \phi_x(x,t) \right\},$$

$$\tau(x,t) := \frac{1}{2b} \int_{-b}^{b} T_{12}(x,y,t)\, dy,$$

$$\tau^b(x,t) := \frac{1}{2b} \int_{-b}^{b} \frac{\partial \eta}{\partial \phi}(x,y,t)\, dy, \quad \tau^\psi(x,t) := \frac{1}{2b} \int_{-b}^{b} \frac{\partial \psi}{\partial \phi}(x,y,t)\, dy,$$

where, τ, τ^b and τ^ψ are the averaged driving force along $\boldsymbol{e}_2$ direction in the layer, due to shear stress, damage energy and elastic energy dependence on plastic strain, respectively. Moreover, B is a non-negative drag coefficient that characterizes the energy dissipation by specifying how the rupture front velocity responds to the applied driving force, locally.

As motivated in Sec. 1, the damage energy density function is assumed to be of the following form:

$$\eta := \mu \frac{\overline{\phi}^2}{\pi^2} \begin{cases} q \left(1 - \cos\left(2\pi \frac{|\phi|}{\overline{\phi}} \right) \right) + R(-\epsilon^e_{22}) \left(1 - \cos\left(2a\pi \frac{|\phi|}{\overline{\phi}} \right) \right), & (\text{for } 0 \le \phi \le \overline{\phi}) \\ 0, & (\text{otherwise}) \end{cases} \tag{10}$$

where, q controls the magnitude of the energetic cost required to induce damage in the fault layer, while a is the frequency of the small perturbations w.r.t. plastic strain/damage. The magnitude of these small perturbations increases with increase in compressive strain, as modeled by the ramp function $R(.)$[2] in (10). Also, $\overline{\phi}$ is the level of plastic strain after which the energetic cost required to induce damage becomes zero. A typical example of the damage energy function was shown earlier in Fig. 2, and the parameters used there for demonstration are: $q = 1$, $a = 20$, with a uniform compressive strain $\epsilon^e_{22} = -0.02$ in fault layer.
Using the expression for η in (10) and for $\boldsymbol{C}_L$ in (7), the expression for driving forces due to damage energy and the dependence of elastic energy on plastic strain are obtained as follows:

$$\frac{\partial \eta}{\partial \phi} = \frac{2\mu\overline{\phi}\, \mathrm{sgn}(\phi)}{\pi} \left\{ q \sin\left(2\pi \frac{|\phi|}{\overline{\phi}} \right) + aR(-\epsilon^e_{22}) \sin\left(2a\pi \frac{|\phi|}{\overline{\phi}} \right) \right\},$$

$$\frac{\partial \psi}{\partial \phi} = -\frac{\kappa}{\overline{\phi}}\, \mathrm{sgn}(\phi) \left\{ \left(\frac{1}{2} \boldsymbol{\epsilon}^e : \boldsymbol{C} : \boldsymbol{\epsilon}^e \right) - (1 - H(\epsilon^e_{22}))\, C_{2222}\, {\epsilon^e_{22}}^2 \right\}.$$

The final set of governing equations in our model are:

$$\rho \frac{\partial^2 u_i}{\partial t^2} = \frac{\partial T_{ij}}{\partial x_j}, \quad (\text{in } \Omega) \tag{11a}$$

$$\phi_t(x,t) = -\phi_x v(x,t), \quad (\text{in } L) \tag{11b}$$

$$v(x,t) := \frac{-1}{B} \left\{ \left[\tau(x,t) - \tau^b(x,t) - \tau^\psi(x,t) + \epsilon \phi_{xx}(x,t) \right] \phi_x(x,t) \right\}. \tag{11c}$$

[2] $R(x)$ is defined as: $R(x) = x$ if $x > 0$, and $R(x) = 0$ if $x <= 0$.

where

$$T_{ij} := \left\{ \begin{array}{c} (C_L)_{ijkl}(u_{k,l} - \phi\,\delta_{k1}\delta_{l2}) - H(-\epsilon^e_{22})\mu\frac{\overline{\phi}^2}{\pi^2}\left(1 - \cos\left(2a\pi\frac{|\phi|}{\overline{\phi}}\right)\right)\delta_{i2}\delta_{j2}, \quad (\text{in } L) \\ C_{ijkl}\,u_{k,l}. \quad (\text{in } \Omega\backslash L) \end{array} \right\}$$

and $\boldsymbol{u}$ is the displacement vector.

Taking b as the fault zone width, and introducing the following non-dimensional variables,

$$\tilde{x} = \frac{x}{b},\ \tilde{t} = \frac{v_s t}{b},\ \tilde{u} = \frac{u}{b},\ \tilde{\boldsymbol{T}} = \frac{\boldsymbol{T}}{\mu},\ \tilde{\boldsymbol{C}} = \frac{\boldsymbol{C}}{\mu},\ \tilde{\tau^b} = \frac{\tau^b}{\mu},\ \tilde{\epsilon} = \frac{\epsilon}{\mu b^2},\ \tilde{B} = \frac{Bb}{\sqrt{\mu\rho}} = \frac{v_s}{\mu/(B\,b)},$$

where $v_s = \sqrt{\mu/\rho}$ is the shear wave speed of the material, and the non-dimensional drag number $\tilde{B}$ represents the ratio of the elastic wave speed of the material to an intrinsic velocity scale of the motion of the rupture front. The non-dimensional form (written without $\tilde{()}$ for simplicity) of the governing equations are:

$$\frac{\partial^2 u_i}{\partial t^2} = \frac{\partial T_{ij}}{\partial x_j}, \quad (\text{in } \Omega) \tag{12a}$$

$$\phi_t(x,t) = \frac{1}{B}\left(\phi_x(x,t)\right)^2\left[\tau(x,t) - \tau^b(x,t) - \tau^\psi(x,t) + \epsilon\phi_{xx}(x,t)\right] \quad (\text{in } L). \tag{12b}$$

The center of the rupture front ϕ profile is defined as the point corresponding to the maximum value of ϕ_x in the fault layer and its displacement is denoted by u^c. Dimensional analysis suggests the following dependence of u^c on the non-dimensional parameter ratios of the model:

$$\frac{u^c}{b} = f^*\left(q, a, \frac{\lambda}{\mu}, \kappa, \tilde{\lambda}, \frac{\sigma_{ap}}{\mu}, \frac{\tau_{ap}}{\mu}, \frac{\epsilon}{\mu b^2}, \frac{Bb}{\sqrt{\mu\rho}}\right),$$

where σ_{ap} and τ_{ap} are the applied compressive and shear stress, respectively.

3 Numerical Scheme

The numerical scheme used for solving the governing equations in our model is a mixed finite element method (FEM) and finite volume method (FVM) based technique. FEM is used for solving the linear momentum balance equation, while a FVM based scheme is used for solving the H-J equation. The grid points for the FVM scheme in the fault layer are taken at the centers of elements of the FEM mesh. The algorithm used here is shown below:

1. For a given initial profile of ϕ, an initial condition for u is obtained by solving $div\,\boldsymbol{T} = \boldsymbol{0}$ using the Galerkin FEM.

2. Assuming fields such as ϕ^t, $\boldsymbol{u}^t$ are known at a given time t.

3. $\phi^{(t+\Delta t)}$ is solved using central upwind scheme [KNP01]. The convection terms are treated explicitly while the diffusion term is implicitly integrated.

4. Displacement solve:

   - For the quasi-static problem, $\boldsymbol{u}^{t+\Delta t}$ is obtained by solving $div\,\boldsymbol{T} = \boldsymbol{0}$ using Galerkin FEM.

- For the dynamic problem, $\boldsymbol{u}^{t+\Delta t}$ is obtained by solving $div\boldsymbol{T} = \rho\ddot{\boldsymbol{u}}$ using Newmark explicit time integration.
- The stiffness matrix for $\boldsymbol{u}^{t+\Delta t}$ solve (both cases) is formed based on $\phi^{t+\Delta t}$.

5. The steps from 2 to 4 are repeated until desired or when equilibrium is achieved for a desired tolerance on ϕ solve.

- Time increment used is, $\Delta t = \min(\Delta t_{\text{cfl}}, \Delta t_{\text{source}}, \Delta t_{\text{dynamic}})$, where

$$\Delta t_{\text{cfl}} = 0.125\frac{\Delta h_x}{\max(|w(x_h)|)}, \quad \Delta t_{\text{source}} = 0.1\frac{B}{\max(|s(x_h)|)},$$
$$\Delta t_{\text{dynamic}} = 0.5\frac{\Delta h_x}{\sqrt{\frac{\lambda+2\mu}{\rho}}}, \quad \text{(only for dynamic case)},$$

and

$$\begin{aligned} w(x_h) &= 2\left(\frac{-\text{sgn}(\phi_x(x_h))}{B}\right)|\phi_x(x_h)|\left[\tau(x_h) - \tau^b(x_h) - \tau^\psi(x_h)\right], \\ s(x_h) &= |\phi_x(x_h)|^2\left(\frac{\partial\tau}{\partial\phi}(x_h) - \frac{\partial\tau^b}{\partial\phi}(x_h) - \frac{\partial\tau^\psi}{\partial\phi}(x_h)\right). \end{aligned}$$

Here, x_h is x coordinate of grid points for ϕ solve, Δh_x is the minimum spacing in x direction in fault layer, while $w(x_h)$ is the linearised front velocity for the rupture front, and $s(x_h)$ is the source term, both obtained from the linearisation of the evolution equation for ϕ.

4 Results and Discussion

We study fault friction numerically using our mathematical model. We apply different levels of compressive stress at the boundary, and thresholds in shear stress are obtained, beyond which the rupture front starts to propagate in the fault layer. Both the compressive stress and shear stress are applied as traction boundary conditions.

4.1 Simulation details

The simulation protocols for a given set of input parameters is as follows:

1. Quasi-static equilibrium is obtained without putting any external loads and equilibrated ϕ profile obtained.

2. The equilbriated ϕ profile from Step 1 is taken as the initial condition, and different levels of normal stresses are applied. Quasi-static equilibrium corresponding to different normal stresses is obtained.

3. The equilbriated ϕ profile corresponding to each normal stress case from Step 2 is taken as the initial condition, and different levels of shear stresses are applied. The highest level of shear stress for which the equilibrium is obtained is taken as the threshold in shear stress, corresponding to a given normal stress.

A given state is called equilibriated if the norm of rate of change of ϕ with respect to time becomes less than an arbitrarily set tolerance, and with this equilibriated ϕ, the norm of change in displacement ($\Delta \boldsymbol{u}$) also becomes less than an arbitrary tolerance. The tolerance value taken for norm of $\dot{\phi}$ is 10^{-3}, while the tolerance value for norm of $\Delta \boldsymbol{u}$ is 10^{-5}. It is also observed for these conditions that the center of the ϕ profile has not moved.

The non-dimensional domain size, fault layer width and mesh size for our simulations are shown in Table 1.

Length	H	W	l	Δh_x	Δh_y
Value	100	100	2	0.25	0.25

Table 1: Domain size, fault-layer width and mesh size used for simulations.

The parameters used for all simulations here are given in Table 2. The only parameter that changes for different simulations is κ, depending upon the amount of elastic damage allowed in the wake of the rupture front in the fault layer.

Parameter	q	a	ϵ	μ	λ	$\tilde{\lambda}$	$\overline{\phi}$
Value	5	500	10	1	2.25	0.7	0.5

Table 2: Parameters used for simulations.

4.2 Emergent fault friction

Based on the protocol mentioned above, we obtain thresholds in shear stress for different normal stresses. In our model, there is competition between different energetic driving forces to prevent or cause the motion, and this leads to thresholds for motion of the rupture front. The driving force from the damage energy function prevents the motion of front, while the averaged shear stress and strain energy terms cause the motion of front. The envelope obtained for the threshold shear stress and the corresponding compressive stress from our simulations resembles the textbook picture of failure envelope for rocks based on experimental observations, as shown in Figure 3. Upon fitting

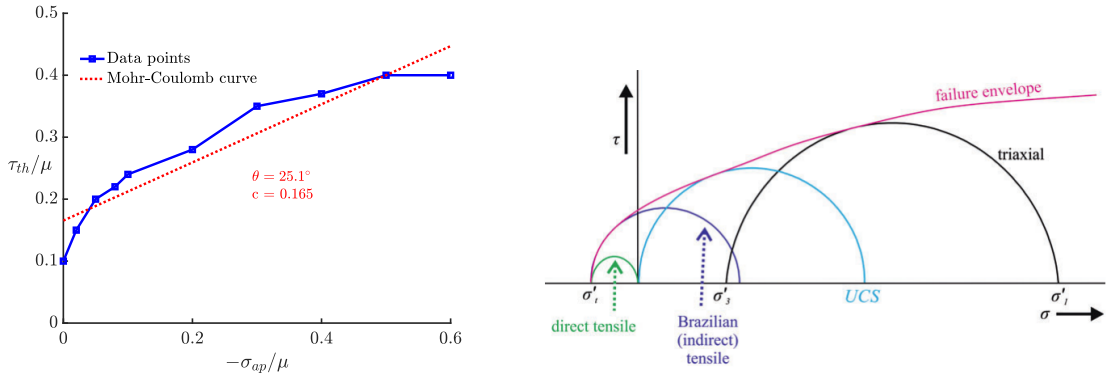

(a) (b)

Figure 3: (a) Shear stress thresholds (τ_{th}/μ) and the corresponding compressive stress ($-\sigma_{ap}/\mu$) obtained for crack-like model ($\kappa = 0.695$), (b) Textbook picture of failure envelope for rocks based on experimental observations [Hac18].

the data points from our simulation results with a linear curve (that resembles a Mohr-Coulomb failure curve), we predict material constants for rocks as shown in Table 3. The cohesion value

Cohesion (c)	$0.165\,\mu$
Friction angle (θ)	25.1°

Table 3: Prediction of material constants from our simulations for crack-like model ($\kappa = 0.695$).

obtained is correlated with the height of the damage energy function (η), which is controlled by q, while the friction angle value obtained is correlated to the frequency of small perturbations in damage energy, which is controlled by a.

5 Conclusion

In this work, we have developed a mathematical model for studying fault friction in dynamic rupture. Without putting in by hand any such criterion in our model, we are able to obtain static fault friction laws from our simulations. We also make a quantitative prediction of material constants for rocks like cohesion and friction angle. We are working with a lesser elastic damage limit in our model, and want to probe whether we can get both fault friction and short-slip predictions, through our simulations.

It will be interesting to work with a model where the rupture front is allowed to move via unrestricted paths in 2-d, within the planar setting that we have used in this paper. In this case, the scalar H-J equation becomes a multi-D system of H-J equations. However, solving a system of H-J equations is a very challenging task, as no rigorous theory or computational schemes for such equations exist in mathematical literature, to our knowledge.

A natural extension of this planar setting is in 3-d, where a 2-d fault layer is surrounded by 3-d elastic blocks, and the scalar 1-d H-J equation becomes a scalar multi-d equation, which can be solved relatively easily by extending the numerical schemes used in this paper.

Acknowledgments

This work was supported by the grant NSF OIA-DMR #2021019.

References

[Ach11] Amit Acharya. Microcanonical entropy and mesoscale dislocation mechanics and plasticity. *Journal of Elasticity*, 104(1):23–44, 2011.

[Ach18] Amit Acharya. Fracture and singularities of the mass-density gradient field. *Journal of Elasticity*, 132(2):243–260, 2018.

[Beh15] R. P Behringer. Jamming in granular materials. *Comptes Rendus Physique*, 16(1):10–25, 2015.

[Bru70] J. N. Brune. Tectonic stress and the spectra of seismic shear waves from earthquakes. *Journal of Geophysical Research*, 75(26):4997–5009, 1970.

[CS79] P. A. Cundall and O. D. L. Strack. A discrete numerical model for granular assemblies. *Geotechnique*, 29(1):47–65, 1979.

[Hac18] R. (H. R. G. K.) Hack. Mohr-coulomb failure envelope. In P. T. Bobrowsky and B. Marker, editors, *Encyclopedia of Engineering Geology*, pages 667–669. Springer International Publishing, Cham, 2018.

[Hea90] T. H. Heaton. Evidence for and implications of self-healing pulses of slip in earthquake rupture. *Physics of the Earth and Planetary Interiors*, 64(1):1–20, 1990.

[HLB18] S. Hulikal, N. Lapusta, and K. Bhattacharya. Static and sliding contact of rough surfaces: effect of asperity-scale properties and long-range elastic interactions. *Journal of the Mechanics and Physics of Solids*, 116:217–238, 2018.

[KNP01] A. Kurganov, S. Noelle, and G. Petrova. Semidiscrete central-upwind schemes for hyperbolic conservation laws and hamilton–jacobi equations. *SIAM Journal on Scientific Computing*, 23(3):707–740, 2001.

[MA21] Léo Morin and Amit Acharya. Analysis of a model of field crack mechanics for brittle materials. *Computer Methods in Applied Mechanics and Engineering*, 386:114061, 2021.

[Mur63] T. Mura. Continuous distribution of moving dislocations. *Philosophical Magazine*, 8(89):843–857, 1963.

[Nab87] F. R. N. Nabarro. *Theory of crystal dislocations*. Dover Publications, 1987.

[Ric01] J. R. Rice. New perspectives on crack and fault dynamics. In *Mechanics for a New Mellennium*, pages 1–24. Springer, 2001.

[RKCH86] A. Ruina, Y. Katzman, G. Conrad, and F. G. Horowitz. Some theory and experiments related to frictional behavior of rocks at low normal stress. *Pure and Applied Geophysics*, pages 1–82, 1986.

[Rui83] A. Ruina. Slip instability and state variable friction laws. *Journal of Geophysical Research: Solid Earth*, 88(B12):10359–10370, 1983.

[ZAWB15] Xiaohan Zhang, Amit Acharya, Noel J. Walkington, and Jacobo Bielak. A single theory for some quasi-static, supersonic, atomic, and tectonic scale applications of dislocations. *Journal of the Mechanics and Physics of Solids*, 84:145–195, 2015.